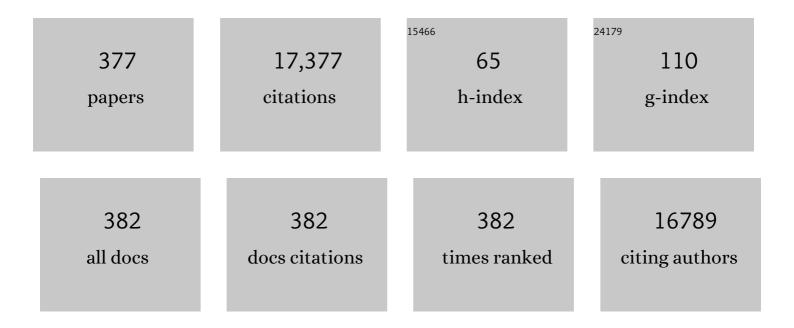
List of Publications by Year in descending order

Source: https://exaly.com/author-pdf/2998750/publications.pdf Version: 2024-02-01



#	Article	IF	CITATIONS
1	Carbon dots: synthesis, formation mechanism, fluorescence origin and sensing applications. Green Chemistry, 2019, 21, 449-471.	4.6	821
2	Highly selective detection of phosphate in very complicated matrixes with an off–on fluorescent probe of europium-adjusted carbon dots. Chemical Communications, 2011, 47, 2604.	2.2	441
3	One-pot hydrothermal synthesis of highly luminescent nitrogen-doped amphoteric carbon dots for bioimaging from Bombyx mori silk – natural proteins. Journal of Materials Chemistry B, 2013, 1, 2868.	2.9	440
4	A general quantitative pH sensor developed with dicyandiamide N-doped high quantum yield graphene quantum dots. Nanoscale, 2014, 6, 3868-3874.	2.8	369
5	Determination of Nucleic Acids by a Resonance Light-Scattering Technique with α,β,γ,δ-Tetrakis[4- (trimethylammoniumyl)phenyl]porphine. Analytical Chemistry, 1996, 68, 2259-2263.	3.2	357
6	Assembly of Aptamer Switch Probes and Photosensitizer on Gold Nanorods for Targeted Photothermal and Photodynamic Cancer Therapy. ACS Nano, 2012, 6, 5070-5077.	7.3	334
7	Visual observation of the mercury-stimulated peroxidase mimetic activity of gold nanoparticles. Chemical Communications, 2011, 47, 11939.	2.2	280
8	Synthesis of Ag Nanocubes 18–32 nm in Edge Length: The Effects of Polyol on Reduction Kinetics, Size Control, and Reproducibility. Journal of the American Chemical Society, 2013, 135, 1941-1951.	6.6	275
9	Curcumin modified silver nanoparticles for highly efficient inhibition of respiratory syncytial virus infection. Nanoscale, 2016, 8, 3040-3048.	2.8	224
10	Synthesis of nitrogen-doping carbon dots with different photoluminescence properties by controlling the surface states. Nanoscale, 2016, 8, 6770-6776.	2.8	214
11	An inner filter effect based sensor of tetracycline hydrochloride as developed by loading photoluminescent carbon nanodots in the electrospun nanofibers. Nanoscale, 2016, 8, 2999-3007.	2.8	194
12	Fluorescent carbon dots functionalization. Advances in Colloid and Interface Science, 2019, 270, 165-190.	7.0	181
13	Polyol Synthesis of Ultrathin Pd Nanowires via Attachmentâ€Based Growth and Their Enhanced Activity towards Formic Acid Oxidation. Advanced Functional Materials, 2014, 24, 131-139.	7.8	173
14	Gold oated Fe ₃ O ₄ Nanoroses with Five Unique Functions for Cancer Cell Targeting, Imaging, and Therapy. Advanced Functional Materials, 2014, 24, 1772-1780.	7.8	172
15	Highly fluorescent carbon dots as selective and visual probes for sensing copper ions in living cells via an electron transfer process. Biosensors and Bioelectronics, 2017, 97, 157-163.	5.3	169
16	Facile in Situ Synthesis of Silver Nanoparticles on the Surface of Metal–Organic Framework for Ultrasensitive Surface-Enhanced Raman Scattering Detection of Dopamine. Analytical Chemistry, 2015, 87, 12177-12182.	3.2	168
17	Chiral nanoprobes for targeting and long-term imaging of the Golgi apparatus. Chemical Science, 2017, 8, 6829-6835.	3.7	167
18	A surfactant-assisted redox hydrothermal route to prepare highly photoluminescent carbon quantum dots with aggregation-induced emission enhancement properties. Chemical Communications, 2013, 49, 8015.	2.2	160

#	Article	IF	CITATIONS
19	Carbon dots synthesized at room temperature for detection of tetracycline hydrochloride. Analytica Chimica Acta, 2019, 1063, 144-151.	2.6	160
20	Synergistic antiviral effect of curcumin functionalized graphene oxide against respiratory syncytial virus infection. Nanoscale, 2017, 9, 16086-16092.	2.8	152
21	Controllable Synthesis of Porphyrinâ€Based 2D Lanthanide Metal–Organic Frameworks with Thickness― and Metalâ€Nodeâ€Dependent Photocatalytic Performance. Angewandte Chemie - International Edition, 2020, 59, 3300-3306.	7.2	148
22	Graphene Signal Amplification for Sensitive and Real-Time Fluorescence Anisotropy Detection of Small Molecules. Analytical Chemistry, 2013, 85, 1424-1430.	3.2	146
23	Toxicity of graphene oxide and multi-walled carbon nanotubes against human cells and zebrafish. Science China Chemistry, 2012, 55, 2209-2216.	4.2	141
24	Large-scale simultaneous synthesis of highly photoluminescent green amorphous carbon nanodots and yellow crystalline graphene quantum dots at room temperature. Green Chemistry, 2017, 19, 3611-3617.	4.6	141
25	Highly selective detection of 2,4,6-trinitrophenol by using newly developed terbium-doped blue carbon dots. Analyst, The, 2016, 141, 2676-2681.	1.7	136
26	One-Step Label-Free Optical Genosensing System for Sequence-Specific DNA Related to the Human Immunodeficiency Virus Based on the Measurements of Light Scattering Signals of Gold Nanorods. Analytical Chemistry, 2008, 80, 8424-8430.	3.2	126
27	One-step synthesis of fluorescent hydroxyls-coated carbon dots with hydrothermal reaction and its application to optical sensing of metal ions. Science China Chemistry, 2011, 54, 1342-1347.	4.2	122
28	Fe3O4 and metal–organic framework MIL-101(Fe) composites catalyze luminol chemiluminescence for sensitively sensing hydrogen peroxide and glucose. Talanta, 2018, 179, 43-50.	2.9	122
29	Real-Time Dark-Field Scattering Microscopic Monitoring of the <i>in Situ</i> Growth of Single Ag@Hg Nanoalloys. ACS Nano, 2013, 7, 11026-11034.	7.3	121
30	In Situ Synthesis of Gold Nanoparticles/Metal–Organic Gels Hybrids with Excellent Peroxidase-Like Activity for Sensitive Chemiluminescence Detection of Organophosphorus Pesticides. ACS Applied Materials & Interfaces, 2018, 10, 28868-28876.	4.0	119
31	Visual and light scattering spectrometric detections of melamine with polythymine-stabilized gold nanoparticles through specific triple hydrogen-bonding recognition. Chemical Communications, 2010, 46, 4893.	2.2	118
32	A large-scale synthesis of photoluminescent carbon quantum dots: a self-exothermic reaction driving the formation of the nanocrystalline core at room temperature. Green Chemistry, 2016, 18, 5127-5132.	4.6	118
33	Photosensitizer–Gold Nanorod Composite for Targeted Multimodal Therapy. Small, 2013, 9, 3678-3684.	5.2	113
34	Redox-Active AIEgen-Derived Plasmonic and Fluorescent Core@Shell Nanoparticles for Multimodality Bioimaging. Journal of the American Chemical Society, 2018, 140, 6904-6911.	6.6	112
35	A colorimetric immunoassay for respiratory syncytial virus detection based on gold nanoparticles–graphene oxide hybrids with mercury-enhanced peroxidase-like activity. Chemical Communications, 2014, 50, 11526-11528.	2.2	106
36	Terbium(III) Modified Fluorescent Carbon Dots for Highly Selective and Sensitive Ratiometry of Stringent. Analytical Chemistry, 2018, 90, 4003-4009.	3.2	106

#	Article	IF	CITATIONS
37	Carbon Nanotubes as a Low Background Signal Platform for a Molecular Aptamer Beacon on the Basis of Long-Range Resonance Energy Transfer. Analytical Chemistry, 2010, 82, 8432-8437.	3.2	104
38	One-pot green synthesis of graphene oxide/gold nanocomposites as SERS substrates for malachite green detection. Analyst, The, 2013, 138, 3075.	1.7	103
39	An Enzyme-Free DNA Circuit-Assisted Graphene Oxide Enhanced Fluorescence Anisotropy Assay for MicroRNA Detection with Improved Sensitivity and Selectivity. Analytical Chemistry, 2017, 89, 8766-8771.	3.2	101
40	Controllable copper deficiency in Cu _{2â^'<i>x</i>} Se nanocrystals with tunable localized surface plasmon resonance and enhanced chemiluminescence. Nanoscale, 2014, 6, 10289-10296.	2.8	100
41	Germanium-doped carbon dots as a new type of fluorescent probe for visualizing the dynamic invasions of mercury(<scp>ii</scp>) ions into cancer cells. Nanoscale, 2015, 7, 16841-16847.	2.8	99
42	Hydrogen-Bond-Mediated <i>in Situ</i> Fabrication of AgNPs/Agar/PAN Electrospun Nanofibers as Reproducible SERS Substrates. ACS Applied Materials & Interfaces, 2015, 7, 1586-1594.	4.0	97
43	Inner filter with carbon quantum dots: A selective sensing platform for detection of hematin in human red cells. Biosensors and Bioelectronics, 2018, 100, 148-154.	5.3	96
44	End-to-end assembly of gold nanorods by means of oligonucleotide–mercury(ii) molecular recognition. Chemical Communications, 2010, 46, 1332.	2.2	93
45	Carbon Nanodots-Catalyzed Chemiluminescence of Luminol: A Singlet Oxygen-Induced Mechanism. Journal of Physical Chemistry C, 2013, 117, 19219-19225.	1.5	90
46	Singlet Oxygen Involved Luminol Chemiluminescence Catalyzed by Graphene Oxide. Journal of Physical Chemistry C, 2012, 116, 21622-21628.	1.5	89
47	A functional preservation strategy for the production of highly photoluminescent emerald carbon dots for lysosome targeting and lysosomal pH imaging. Nanoscale, 2018, 10, 14705-14711.	2.8	86
48	Photothermal Soft Nanoballs Developed by Loading Plasmonic Cu _{2–<i>x</i>} Se Nanocrystals into Liposomes for Photothermal Immunoassay of Aflatoxin B ₁ . Analytical Chemistry, 2019, 91, 4444-4450.	3.2	84
49	Novel Iron(III)-Based Metal–Organic Gels with Superior Catalytic Performance toward Luminol Chemiluminescence. ACS Applied Materials & Interfaces, 2017, 9, 31834-31840.	4.0	83
50	Visual Sandwich Immunoassay System on the Basis of Plasmon Resonance Scattering Signals of Silver Nanoparticles. Analytical Chemistry, 2009, 81, 1707-1714.	3.2	82
51	A graphene oxide enhanced fluorescence anisotropy strategy for DNAzyme-based assay of metal ions. Chemical Communications, 2013, 49, 1942.	2.2	80
52	Dark-Field Microscopy: Recent Advances in Accurate Analysis and Emerging Applications. Analytical Chemistry, 2021, 93, 4707-4726.	3.2	79
53	Green and easy synthesis of biocompatible graphene for use as an anticoagulant. RSC Advances, 2012, 2, 2322.	1.7	78
54	A distance-dependent metal-enhanced fluorescence sensing platform based on molecular beacon design. Biosensors and Bioelectronics, 2014, 52, 367-373.	5.3	78

#	Article	IF	CITATIONS
55	One-step synthesis of chiral carbon quantum dots and their enantioselective recognition. RSC Advances, 2016, 6, 59956-59960.	1.7	78
56	An active structure preservation method for developing functional graphitic carbon dots as an effective antibacterial agent and a sensitive pH and Al(<scp>iii</scp>) nanosensor. Nanoscale, 2017, 9, 17334-17341.	2.8	76
57	Screening sensitive nanosensors via the investigation of shape-dependent localized surface plasmon resonance of single Ag nanoparticles. Nanoscale, 2013, 5, 7458.	2.8	75
58	Photoinduced Electron Transfer Process Visualized on Single Silver Nanoparticles. ACS Nano, 2017, 11, 2085-2093.	7.3	75
59	One-pot carbonization synthesis of europium-doped carbon quantum dots for highly selective detection of tetracycline. Methods and Applications in Fluorescence, 2017, 5, 015003.	1.1	75
60	Carbon dots with aggregation induced emission enhancement for visual permittivity detection. Chemical Communications, 2016, 52, 2063-2066.	2.2	74
61	Carbon dot-based composites for catalytic applications. Green Chemistry, 2020, 22, 4034-4054.	4.6	74
62	A graphitic carbon nitride based fluorescence resonance energy transfer detection of riboflavin. Talanta, 2016, 148, 279-284.	2.9	72
63	Photoluminescence of carbon quantum dots: coarsely adjusted by quantum confinement effects and finely by surface trap states. Science China Chemistry, 2018, 61, 490-496.	4.2	72
64	Controlled synthesis of CuS caved superstructures and their application to the catalysis of organic dye degradation in the absence of light. CrystEngComm, 2015, 17, 1374-1380.	1.3	70
65	Gold nanoparticles immobilized on metal–organic frameworks with enhanced catalytic performance for DNA detection. Analytica Chimica Acta, 2015, 861, 55-61.	2.6	69
66	Aggregation-induced emission enhancement of yellow photoluminescent carbon dots for highly selective detection of environmental and intracellular copper(II) ions. Chinese Chemical Letters, 2019, 30, 1410-1414.	4.8	69
67	CuO nanoparticles derived from metal-organic gel with excellent electrocatalytic and peroxidase-mimicking activities for glucose and cholesterol detection. Biosensors and Bioelectronics, 2019, 145, 111704.	5.3	68
68	A facile and green method to fabricate graphene-based multifunctional hydrogels for miniature-scale water purification. RSC Advances, 2013, 3, 9240.	1.7	65
69	Cu(<scp>i</scp>)-Doped carbon quantum dots with zigzag edge structures for highly efficient catalysis of azide–alkyne cycloadditions. Green Chemistry, 2017, 19, 1494-1498.	4.6	65
70	Electrostatic Assemblies of Well-Dispersed AgNPs on the Surface of Electrospun Nanofibers as Highly Active SERS Substrates for Wide-Range pH Sensing. ACS Applied Materials & Interfaces, 2016, 8, 14802-14811.	4.0	64
71	Anthrax biomarker: An ultrasensitive fluorescent ratiometry of dipicolinic acid by using terbium(III)-modified carbon dots. Talanta, 2019, 191, 443-448.	2.9	64
72	Terbium(III) Organic Gels: Novel Antenna Effect-Induced Enhanced Electrochemiluminescence Emitters. Analytical Chemistry, 2018, 90, 12191-12197.	3.2	63

#	Article	IF	CITATIONS
73	Antibacterials loaded electrospun composite nanofibers: release profile and sustained antibacterial efficacy. Polymer Chemistry, 2014, 5, 1965-1975.	1.9	62
74	Functional preserving carbon dots-based fluorescent probe for mercury (II) ions sensing in herbal medicines via coordination and electron transfer. Analytica Chimica Acta, 2018, 1035, 203-210.	2.6	60
75	Energy transfer with gold nanoparticles for analytical applications in the fields of biochemical and pharmaceutical sciences. Analytical Methods, 2010, 2, 1439.	1.3	59
76	Graphene oxide as an efficient signal-to-background enhancer for DNA detection with a long range resonance energy transfer strategy. Chemical Communications, 2011, 47, 11718.	2.2	59
77	A highly selective and colorimetric assay of lysine by molecular-driven gold nanorods assembly. Biosensors and Bioelectronics, 2012, 34, 197-201.	5.3	59
78	An enzyme-induced Au@Ag core–shell nanoStructure used for an ultrasensitive surface-enhanced Raman scattering immunoassay of cancer biomarkers. Nanoscale, 2017, 9, 2640-2645.	2.8	59
79	Self-exothermic reaction prompted synthesis of single-layered graphene quantum dots at room temperature. Chemical Communications, 2017, 53, 4958-4961.	2.2	59
80	Silver nanoparticles deposited on graphene oxide for ultrasensitive surface-enhanced Raman scattering immunoassay of cancer biomarker. Nanoscale, 2018, 10, 11942-11947.	2.8	59
81	Ultrasensitive Electrochemiluminescence Detection of MicroRNA via One-Step Introduction of a Target-Triggered Branched Hybridization Chain Reaction Circuit. Analytical Chemistry, 2019, 91, 9308-9314.	3.2	59
82	Visually monitoring the etching process of gold nanoparticles by KI/I2 at single-nanoparticle level using scattered-light dark-field microscopic imaging. Nano Research, 2016, 9, 1125-1134.	5.8	58
83	DNA Nanofirecrackers Assembled through Hybridization Chain Reaction for Ultrasensitive SERS Immunoassay of Prostate Specific Antigen. Analytical Chemistry, 2020, 92, 4046-4052.	3.2	56
84	Aptamer-Mediated Nanoparticle-Based Protein Labeling Platform for Intracellular Imaging and Tracking Endocytosis Dynamics. Analytical Chemistry, 2012, 84, 3099-3110.	3.2	55
85	Optically active red-emitting Cu nanoclusters originating from complexation and redox reaction between copper(<scp>ii</scp>) and <scp>d</scp> / <scp>l</scp> -penicillamine. Nanoscale, 2016, 8, 9764-9770.	2.8	55
86	Localized surface plasmon resonance of gold nanorods and assemblies in the view of biomedical analysis. TrAC - Trends in Analytical Chemistry, 2016, 80, 429-443.	5.8	55
87	Ru(III)-Based Metal–Organic Gels: Intrinsic Horseradish and NADH Peroxidase-Mimicking Nanozyme. ACS Applied Materials & Interfaces, 2019, 11, 29158-29166.	4.0	55
88	Individually color-coded plasmonic nanoparticles for RGB analysis. Chemical Communications, 2011, 47, 8121.	2.2	54
89	Real-Time Light Scattering Tracking of Gold Nanoparticles- bioconjugated Respiratory Syncytial Virus Infecting HEp-2 Cells. Scientific Reports, 2014, 4, 4529.	1.6	54
90	Dendritic CuSe with Hierarchical Side-Branches: Synthesis, Efficient Adsorption, and Enhanced Photocatalytic Activities under Daylight. ACS Sustainable Chemistry and Engineering, 2017, 5, 4154-4160.	3.2	54

#	Article	IF	CITATIONS
91	Recent Developments of the Resonance Light Scattering Technique: Technical Evolution, New Probes and Applications. Applied Spectroscopy Reviews, 2007, 42, 177-201.	3.4	51
92	Highly selective and sensitive detection of 2,4,6-trinitrophenol by using newly developed blue–green photoluminescent carbon nanodots. Talanta, 2016, 161, 875-880.	2.9	51
93	Stable gold nanoparticles as a novel peroxidase mimic for colorimetric detection of cysteine. Analytical Methods, 2016, 8, 2494-2501.	1.3	51
94	Highly selective detection of phosphate ion based on a single-layered graphene quantum dots-Al3+ strategy. Talanta, 2018, 178, 172-177.	2.9	51
95	Mitochondria-targeting single-layered graphene quantum dots with dual recognition sites for ATP imaging in living cells. Nanoscale, 2018, 10, 17402-17408.	2.8	51
96	Recent insights into functionalized electrospun nanofibrous films for chemo-/bio-sensors. TrAC - Trends in Analytical Chemistry, 2020, 124, 115813.	5.8	51
97	Polarity-Sensitive Polymer Carbon Dots Prepared at Room-Temperature for Monitoring the Cell Polarity Dynamics during Autophagy. ACS Applied Materials & Interfaces, 2020, 12, 4815-4820.	4.0	50
98	Facile synthesis of binary two-dimensional lanthanide metal-organic framework nanosheets for ratiometric fluorescence detection of mercury ions. Journal of Hazardous Materials, 2022, 423, 126978.	6.5	50
99	A portable RGB sensing gadget for sensitive detection of Hg2+ using cysteamine-capped QDs as fluorescence probe. Biosensors and Bioelectronics, 2017, 98, 36-40.	5.3	49
100	Carbon dotsâ€involved chemiluminescence: Recent advances and developments. Luminescence, 2019, 34, 4-22.	1.5	49
101	Carbon dots as nanocatalytic medicine for anti-inflammation therapy. Journal of Colloid and Interface Science, 2022, 611, 545-553.	5.0	49
102	Water-soluble luminescent copper nanoclusters reduced and protected by histidine for sensing of guanosine 5′-triphosphate. New Journal of Chemistry, 2014, 38, 3673.	1.4	48
103	Boron and nitrogen co-doped single-layered graphene quantum dots: a high-affinity platform for visualizing the dynamic invasion of HIV DNA into living cells through fluorescence resonance energy transfer. Journal of Materials Chemistry B, 2017, 5, 8719-8724.	2.9	48
104	2D MOF-Based Photoelectrochemical Aptasensor for SARS-CoV-2 Spike Glycoprotein Detection. ACS Applied Materials & Interfaces, 2021, 13, 49754-49761.	4.0	48
105	Luminescent golden silk and fabric through in situ chemically coating pristine-silk with gold nanoclusters. Biomaterials, 2015, 36, 26-32.	5.7	47
106	Surface-engineered quantum dots/electrospun nanofibers as a networked fluorescence aptasensing platform toward biomarkers. Nanoscale, 2017, 9, 17020-17028.	2.8	47
107	Color-Encoded Assays for the Simultaneous Quantification of Dual Cancer Biomarkers. Analytical Chemistry, 2017, 89, 8484-8489.	3.2	47
108	Core-shell quantum dots coated with molecularly imprinted polymer for selective photoluminescence sensing of perfluorooctanoic acid. Talanta, 2019, 194, 1-6.	2.9	47

#	Article	IF	CITATIONS
109	Use of the peroxidase mimetic activity of erythrocyte-like Cu _{1.8} S nanoparticles in the colorimetric determination of glutathione. Analytical Methods, 2017, 9, 841-846.	1.3	46
110	Ratiometrically Fluorescent Electrospun Nanofibrous Film as a Cu ²⁺ -Mediated Solid-Phase Immunoassay Platform for Biomarkers. Analytical Chemistry, 2018, 90, 9966-9974.	3.2	46
111	Shape- and size-dependent catalysis activities of iron-terephthalic acid metal-organic frameworks. Science China Chemistry, 2015, 58, 1553-1560.	4.2	45
112	Preparation of nitrogen-doped carbon dots with high quantum yield from Bombyx mori silk for Fe(<scp>iii</scp>) ions detection. RSC Advances, 2017, 7, 50584-50590.	1.7	45
113	Identification of Iodine-Induced Morphological Transformation of Gold Nanorods. Journal of Physical Chemistry C, 2008, 112, 11691-11695.	1.5	44
114	Graphene oxide as a nano-platform for ATP detection based on aptamer chemistry. Analytical Methods, 2012, 4, 1662.	1.3	44
115	"Click―on Alkynylated Carbon Quantum Dots: An Efficient Surface Functionalization for Specific Biosensing and Bioimaging. Chemistry - A European Journal, 2017, 23, 2171-2178.	1.7	44
116	Development of nitrogen and sulfur-doped carbon dots for cellular imaging. Journal of Pharmaceutical Analysis, 2019, 9, 127-132.	2.4	44
117	Resonance light scattering imaging detection of proteins with α,β,γ,δ-tetrakis(p-sulfophenyl)porphyrin. Analytical Biochemistry, 2003, 321, 236-243.	1.1	43
118	Label-free and selective sensing of uric acid with gold nanoclusters as optical probe. Talanta, 2016, 152, 314-320.	2.9	43
119	A sensitive surface-enhanced Raman scattering enzyme-catalyzed immunoassay of respiratory syncytial virus. Talanta, 2016, 148, 308-312.	2.9	43
120	Dynamically Long-Term Imaging of Cellular RNA by Fluorescent Carbon Dots with Surface Isoquinoline Moieties and Amines. Analytical Chemistry, 2018, 90, 11358-11365.	3.2	43
121	Pt-Cr2O3-WO3 composite nanofibers as gas sensors for ultra-high sensitive and selective xylene detection. Sensors and Actuators B: Chemical, 2019, 300, 127008.	4.0	43
122	The aggregation induced emission quenching of graphene quantum dots for visualizing the dynamic invasions of cobalt(<scp>ii</scp>) into living cells. Journal of Materials Chemistry B, 2017, 5, 6394-6399.	2.9	42
123	Enzyme Activity Triggered Blocking of Plasmon Resonance Energy Transfer for Highly Selective Detection of Acid Phosphatase. Analytical Chemistry, 2020, 92, 2130-2135.	3.2	42
124	Porous hollow CuS nanospheres with prominent peroxidase-like activity prepared in large scale by a one-pot controllable hydrothermal step. RSC Advances, 2015, 5, 17458-17465.	1.7	41
125	Real-time dark-field light scattering imaging to monitor the coupling reaction with gold nanorods as an optical probe. Nanoscale, 2017, 9, 3568-3575.	2.8	41
126	Metal–organic framework MIL-101 enhanced fluorescence anisotropy for sensitive detection of DNA. RSC Advances, 2014, 4, 9379-9382.	1.7	40

#	Article	IF	CITATIONS
127	General Sensitive Detecting Strategy of Ions through Plasmonic Resonance Energy Transfer from Gold Nanoparticles to Rhodamine Spirolactam. Analytical Chemistry, 2017, 89, 1808-1814.	3.2	40
128	Branched polyethylenimine-functionalized carbon dots as sensitive and selective fluorescent probes for N-acetylcysteine via an off–on mechanism. Analyst, The, 2017, 142, 4221-4227.	1.7	40
129	One-pot preparation of dextran-capped gold nanoparticles at room temperature and colorimetric detection of dihydralazine sulfate in uric samples. Analytical Methods, 2010, 2, 1982.	1.3	39
130	Fluorescent detection of silver(I) and cysteine using SYBR Green I and a silver(I)-specific oligonucleotide. Mikrochimica Acta, 2012, 177, 137-144.	2.5	39
131	Highly selective detection of bacterial alarmone ppGpp with an off–on fluorescent probe of copper-mediated silver nanoclusters. Biosensors and Bioelectronics, 2013, 49, 433-437.	5.3	39
132	Gold nanoparticle-based enhanced ELISA for respiratory syncytial virus. New Journal of Chemistry, 2014, 38, 2935-2940.	1.4	39
133	HSI colour-coded analysis of scattered light of single plasmonic nanoparticles. Nanoscale, 2016, 8, 11467-11471.	2.8	39
134	Protective effect of Dendrobium officinale polysaccharides on H2O2-induced injury in H9c2 cardiomyocytes. Biomedicine and Pharmacotherapy, 2017, 94, 72-78.	2.5	39
135	Zinc–Metal Organic Frameworks: A Coreactant-free Electrochemiluminescence Luminophore for Ratiometric Detection of miRNA-133a. Analytical Chemistry, 2021, 93, 14178-14186.	3.2	39
136	Fluorescent carbon dots: facile synthesis at room temperature and its application for Fe2+ sensing. Journal of Nanoparticle Research, 2017, 19, 1.	0.8	38
137	Recent advances of carbon dots in imaging-guided theranostics. TrAC - Trends in Analytical Chemistry, 2021, 134, 116116.	5.8	38
138	Controllable preparation of metal nanoparticle/carbon nanotube hybrids as efficient dark field light scattering agents for cell imaging. Chemical Communications, 2010, 46, 4303.	2.2	37
139	Graphene oxide amplified fluorescence anisotropy for label-free detection of potassium ion. Analyst, The, 2015, 140, 353-357.	1.7	37
140	Cytosine triphosphate-capped silver nanoparticles as a platform for visual and colorimetric determination of mercury(II) and chromium(III). Mikrochimica Acta, 2017, 184, 3171-3178.	2.5	37
141	Plasmonics-attended NSET and PRET for analytical applications. TrAC - Trends in Analytical Chemistry, 2020, 124, 115805.	5.8	37
142	A novel graphene oxide amplified fluorescence anisotropy assay with improved accuracy and sensitivity. Chemical Communications, 2015, 51, 16080-16083.	2.2	36
143	Real-time monitoring of oxidative etching on single Ag nanocubes via light-scattering dark-field microscopy imaging. Nanoscale, 2015, 7, 15209-15213.	2.8	36
144	A graphene oxide-based strand displacement amplification platform for ricin detection using aptamer as recognition element. Biosensors and Bioelectronics, 2017, 91, 149-154.	5.3	36

#	Article	IF	CITATIONS
145	Carbon dots-based fluorescence resonance energy transfer for the prostate specific antigen (PSA) with high sensitivity. Talanta, 2020, 219, 121276.	2.9	36
146	Plasmon-induced light concentration enhanced imaging visibility as observed by a composite-field microscopy imaging system. Chemical Science, 2016, 7, 5477-5483.	3.7	35
147	Exonuclease III-assisted graphene oxide amplified fluorescence anisotropy strategy for ricin detection. Biosensors and Bioelectronics, 2016, 85, 822-827.	5.3	35
148	New Off–On Sensor for Captopril Sensing Based on Photoluminescent MoO <i>_x</i> Quantum Dots. ACS Omega, 2017, 2, 1666-1671.	1.6	35
149	Carbon Quantum Dots–Europium(III) Energy Transfer Architecture Embedded in Electrospun Nanofibrous Membranes for Fingerprint Security and Document Counterspy. Analytical Chemistry, 2019, 91, 11185-11191.	3.2	35
150	Hydrophilic Cu2â^'xSe/reduced graphene oxide nanocomposites with tunable plasmonic properties and their applications in cellular dark-field microscopic imaging. Journal of Materials Chemistry B, 2014, 2, 7027-7033.	2.9	34
151	Nanosilver-based surface-enhanced Raman spectroscopic determination of DNA methyltransferase activity through real-time hybridization chain reaction. Biosensors and Bioelectronics, 2015, 73, 228-233.	5.3	34
152	Cobalt oxyhydroxide nanoflakes with oxidase-mimicking activity induced chemiluminescence of luminol for glutathione detection. Talanta, 2020, 215, 120928.	2.9	34
153	Hierarchical Hybridization Chain Reaction for Amplified Signal Output and Cascade DNA Logic Circuits. Analytical Chemistry, 2021, 93, 3411-3417.	3.2	34
154	DNA-AuNP networks on cell membranes as a protective barrier to inhibit viral attachment, entry and budding. Biomaterials, 2016, 77, 216-226.	5.7	33
155	A cancer-targeted drug delivery system developed with gold nanoparticle mediated DNA–doxorubicin conjugates. RSC Advances, 2014, 4, 34830-34835.	1.7	32
156	Luminol and gold nanoparticle-co-precipitated reduced graphene oxide hybrids with long-persistent chemiluminescence for cholesterol detection. Journal of Materials Chemistry B, 2017, 5, 7335-7341.	2.9	32
157	Silver-based metal-organic gels as novel coreactant for enhancing electrochemiluminescence and its biosensing potential. Biosensors and Bioelectronics, 2019, 134, 29-35.	5.3	32
158	Lattice expansion and oxygen vacancy of α-Fe2O3 during gas sensing. Talanta, 2021, 221, 121616.	2.9	32
159	Self-Targeting Carbon Quantum Dots for Peroxynitrite Detection and Imaging in Live Cells. Analytical Chemistry, 2021, 93, 16466-16473.	3.2	32
160	Electrochemiluminescence Resonance Energy Transfer System Based on Silver Metal–Organic Frameworks as a Double-Amplified Emitter for Sensitive Detection of miRNA-107. Analytical Chemistry, 2022, 94, 1178-1186.	3.2	32
161	DNA Logic Nanodevices for the Sequential Imaging of Cancer Markers through Localized Catalytic Hairpin Assembly Reaction. Analytical Chemistry, 2022, 94, 4399-4406.	3.2	32
162	A resonance light scattering ratiometry applied for binding study of organic small molecules with biopolymer. Talanta, 2006, 69, 180-186.	2.9	31

#	Article	IF	CITATIONS
163	Sensitive detection of prion protein through long range resonance energy transfer between graphene oxide and molecular aptamer beacon. Analytical Methods, 2013, 5, 208-212.	1.3	31
164	Aptamer-mediated nanocomposites of semiconductor quantum dots and graphene oxide as well as their applications in intracellular imaging and targeted drug delivery. Journal of Materials Chemistry B, 2014, 2, 8558-8565.	2.9	31
165	Aluminum-doped NiO nanofibers as chemical sensors for selective and sensitive methanol detection. Analytical Methods, 2019, 11, 575-581.	1.3	31
166	Nitrogen and phosphorus doped polymer carbon dots as a sensitive cellular mapping probe of nitrite. Journal of Materials Chemistry B, 2019, 7, 2074-2080.	2.9	31
167	Controllable Synthesis of Porphyrinâ€Based 2D Lanthanide Metal–Organic Frameworks with Thickness― and Metalâ€Nodeâ€Dependent Photocatalytic Performance. Angewandte Chemie, 2020, 132, 3326-3332.	1.6	31
168	An efficient solid-state synthesis of fluorescent surface carboxylated carbon dots derived from C60 as a label-free probe for iron ions in living cells. Talanta, 2015, 144, 93-97.	2.9	30
169	Plasmonic platforms for colorimetric sensing of cysteine. Applied Spectroscopy Reviews, 2016, 51, 129-147.	3.4	30
170	Dual Energy Transfer-Based Fluorescent Nanoprobe for Imaging miR-21 in Nonalcoholic Fatty Liver Cells with Low Background. Analytical Chemistry, 2019, 91, 6761-6768.	3.2	30
171	Development of a portable device for Ag+ sensing using CdTe QDs as fluorescence probe via an electron transfer process. Talanta, 2019, 191, 357-363.	2.9	30
172	High-Resolution Vertical Polarization Excited Dark-Field Microscopic Imaging of Anisotropic Gold Nanorods for the Sensitive Detection and Spatial Imaging of Intracellular microRNA-21. Analytical Chemistry, 2020, 92, 13118-13125.	3.2	30
173	DNA-templated silver nanoclusters as label-free fluorescent probes for detection of bleomycin. Analytical Methods, 2013, 5, 6200.	1.3	29
174	Reduced graphene oxide gated mesoporous silica nanoparticles as a versatile chemo-photothermal therapy system through pH controllable release. Journal of Materials Chemistry B, 2015, 3, 6377-6384.	2.9	29
175	Synergetic Catalytic Effect of Cu2–xSe Nanoparticles and Reduced Graphene Oxide Coembedded in Electrospun Nanofibers for the Reduction of a Typical Refractory Organic Compound. ACS Applied Materials & Interfaces, 2015, 7, 15447-15457.	4.0	29
176	A 2D MOF-based artificial light-harvesting system with chloroplast bionic structure for photochemical catalysis. Journal of Materials Chemistry A, 2021, 9, 9301-9306.	5.2	29
177	Cu vacancies enhanced photoelectrochemical activity of metal-organic gel-derived CuO for the detection of l-cysteine. Talanta, 2021, 228, 122261.	2.9	29
178	Morphology Control and Structural Characterization of Au Crystals: From Twinned Tabular Crystals and Single-Crystalline Nanoplates to Multitwinned Decahedra. Crystal Growth and Design, 2009, 9, 3211-3217.	1.4	28
179	Facile synthesis of a Fe ₃ O ₄ /MIL-101(Fe) composite with enhanced catalytic performance. RSC Advances, 2016, 6, 86443-86446.	1.7	28
180	Plasmonic Cu _{2–<i>x</i>} S _{<i>y</i>} Se _{1–<i>y</i>} Nanoparticles Catalyzed Click Chemistry Reaction for SERS Immunoassay of Cancer Biomarker. Analytical Chemistry, 2018, 90, 11728-11733.	3.2	28

#	Article	IF	CITATIONS
181	Rational Design of pHâ€Responsive DNA Motifs with General Sequence Compatibility. Angewandte Chemie - International Edition, 2019, 58, 16405-16410.	7.2	28
182	Dual Energy Transfer-Based DNA/Graphene Oxide Nanocomplex Probe for Highly Robust and Accurate Monitoring of Apoptosis-Related microRNAs. Analytical Chemistry, 2020, 92, 11565-11572.	3.2	28
183	Label-free DNA detection on the basis of fluorescence resonance energy transfer from oligonucleotide-templated silver nanoclusters to multi-walled carbon nanotubes. Analytical Methods, 2013, 5, 5555.	1.3	27
184	Cu ²⁺ -mediated fluorescence switching of gold nanoclusters for the selective detection of clioquinol. Analyst, The, 2015, 140, 8194-8200.	1.7	27
185	Selective colorimetric analysis of spermine based on the cross-linking aggregation of gold nanoparticles chain assembly. Talanta, 2017, 167, 193-200.	2.9	27
186	A galvanic exchange process visualized on single silver nanoparticles <i>via</i> dark-field microscopy imaging. Nanoscale, 2018, 10, 12805-12812.	2.8	27
187	Label-free gold nanorods sensor array for colorimetric detection and discrimination of biothiols in human urine samples. Talanta, 2019, 203, 220-226.	2.9	27
188	Metal–Organic Gelâ€Derived Multimetal Oxides as Effective Electrocatalysts for the Oxygen Evolution Reaction. ChemSusChem, 2019, 12, 2480-2486.	3.6	27
189	Precision improvement in dark-field microscopy imaging by using gold nanoparticles as an internal reference: a combined theoretical and experimental study. Nanoscale, 2016, 8, 8729-8736.	2.8	26
190	2,4,6-Trinitrophenol detection by a new portable sensing gadget using carbon dots as a fluorescent probe. Analytical and Bioanalytical Chemistry, 2019, 411, 2291-2300.	1.9	26
191	Gold Triangular Nanoplates Based Single-Particle Dark-Field Microscopy Assay of Pyrophosphate. Analytical Chemistry, 2019, 91, 15798-15803.	3.2	26
192	Simultaneous Imaging of Dual microRNAs in Cancer Cells through Catalytic Hairpin Assembly on a DNA Tetrahedron. ACS Applied Materials & Interfaces, 2022, 14, 12059-12067.	4.0	26
193	Polydopamine-embedded Cu _{2â^x} Se nanoparticles as a sensitive biosensing platform through the coupling of nanometal surface energy transfer and photo-induced electron transfer. Analyst, The, 2015, 140, 4121-4129.	1.7	25
194	Luminescent Zn(<scp>ii</scp>)–terpyridine metal–organic gel for visual recognition of anions. RSC Advances, 2015, 5, 2857-2860.	1.7	25
195	Rapid detection of a dengue virus RNA sequence with single molecule sensitivity using tandem toehold-mediated displacement reactions. Chemical Communications, 2018, 54, 968-971.	2.2	25
196	Localized surface plasmon resonance scattering imaging and spectroscopy for real-time reaction monitoring. Applied Spectroscopy Reviews, 2019, 54, 237-249.	3.4	25
197	Green One-Pot Synthesis of Silver Nanoparticles/Metal–Organic Gels Hybrid and Its Promising SERS Application. ACS Sustainable Chemistry and Engineering, 2019, 7, 5292-5299.	3.2	25
198	A copper(II)/cobalt(II) organic gel with enhanced peroxidase-like activity for fluorometric determination of hydrogen peroxide and glucose. Mikrochimica Acta, 2019, 186, 168.	2.5	25

#	Article	IF	CITATIONS
199	Singleâ€Crystalline TiO ₂ (B) Nanobelts with Unusual Large Exposed {100} Facets and Enhanced Liâ€Storage Capacity. Advanced Functional Materials, 2021, 31, 2002187.	7.8	25
200	Automated Plasmonic Resonance Scattering Imaging Analysis via Deep Learning. Analytical Chemistry, 2021, 93, 2619-2626.	3.2	25
201	Highly Sensitive Detection of miR-21 through Target-Activated Catalytic Hairpin Assembly of X-Shaped DNA Nanostructures. Analytical Chemistry, 2021, 93, 14545-14551.	3.2	25
202	Efficient visible-light photocatalytic heterojunctions formed by coupling plasmonic Cu _{2â^'x} Se and graphitic carbon nitride. New Journal of Chemistry, 2015, 39, 6186-6192.	1.4	24
203	Encapsulating a ruthenium(<scp>ii</scp>) complex into metal organic frameworks to engender high sensitivity for dopamine electrochemiluminescence detection. Analytical Methods, 2018, 10, 1560-1564.	1.3	24
204	Metal-organic gel enhanced fluorescence anisotropy for sensitive detection of prostate specific antigen. Spectrochimica Acta - Part A: Molecular and Biomolecular Spectroscopy, 2018, 192, 328-332.	2.0	24
205	Dual-ligand two-dimensional Europium-organic gels nanosheets for ratiometric fluorescence detecting anthrax spore biomarker. Chemical Engineering Journal, 2022, 435, 134912.	6.6	24
206	Polymethacrylic acid–facilitated nanofiber matrix loading Ag nanoparticles for SERS measurements. RSC Advances, 2014, 4, 38783-38790.	1.7	23
207	MIL-101(Cr) as matrix for sensitive detection of quercetin by matrix-assisted laser desorption/ionization mass spectrometry. Talanta, 2017, 164, 355-361.	2.9	23
208	Precise ricin A-chain delivery by Golgi-targeting carbon dots. Chemical Communications, 2019, 55, 6437-6440.	2.2	23
209	Graphitic C3N4 nanosheet and hemin/G-quadruplex DNAzyme-based label-free chemiluminescence aptasensing for biomarkers. Talanta, 2019, 192, 400-406.	2.9	23
210	Rapid and convenient synthesis of stable silver nanoparticles with kiwi juice and its novel application for detecting protease K. New Journal of Chemistry, 2015, 39, 1295-1300.	1.4	22
211	Förster Resonance Energy Transfer-Based Soft Nanoballs for Specific and Amplified Detection of MicroRNAs. Analytical Chemistry, 2019, 91, 11023-11029.	3.2	22
212	One-step synthesis of Cu(II) metal–organic gel as recyclable material for rapid, efficient and size selective cationic dyes adsorption. Journal of Environmental Sciences, 2019, 86, 203-212.	3.2	22
213	Continuous singlet oxygen generation for persistent chemiluminescence in Cu-MOFs-based catalytic system. Talanta, 2021, 221, 121498.	2.9	22
214	Transformable Helical Self-Assembly for Cancerous Golgi Apparatus Disruption. Nano Letters, 2021, 21, 8455-8465.	4.5	22
215	Tuning of the near-infrared localized surface plasmon resonance of Cu _{2â^x} Se nanoparticles with lysozyme-induced selective aggregation. RSC Advances, 2014, 4, 55094-55099.	1.7	21
216	Simple preparation of magnetic metal-organic frameworks composite as a "bait―for phosphoproteome research. Talanta, 2017, 171, 283-290.	2.9	21

#	Article	IF	CITATIONS
217	Individual Plasmonic Nanoprobes for Biosensing and Bioimaging: Recent Advances and Perspectives. Small, 2021, 17, e2004287.	5.2	21
218	Histidine-mediated synthesis of chiral fluorescence gold nanoclusters: insight into the origin of nanoscale chirality. RSC Advances, 2015, 5, 61449-61454.	1.7	20
219	Aggregation-induced superior peroxidase-like activity of Cu _{2â^`x} Se nanoparticles for melamine detection. Analytical Methods, 2016, 8, 7516-7521.	1.3	20
220	A sensitive and low background fluorescent sensing strategy based on g-C ₃ N ₄ –MnO ₂ sandwich nanocomposite and liposome amplification for ricin detection. Analyst, The, 2018, 143, 5764-5770.	1.7	20
221	Highly selective detection of spermine in human urine via a nanometal surface energy transfer platform. Talanta, 2018, 188, 218-224.	2.9	20
222	Selfâ€Assembly of Microparticles by Supramolecular Homopolymerization of One Component DNA Molecule. Small, 2019, 15, e1805552.	5.2	20
223	Ultrasensitive ratiometric electrochemiluminescence for detecting atxA mRNA using luminol-encapsulated liposome as effectively amplified signal labels. Biosensors and Bioelectronics, 2021, 186, 113263.	5.3	20
224	Controlled synthesis of zinc-metal organic framework microflower with high efficiency electrochemiluminescence for miR-21 detection. Biosensors and Bioelectronics, 2022, 213, 114443.	5.3	20
225	Real-time scattered light dark-field microscopic imaging of the dynamic degradation process of sodium dimethyldithiocarbamate. Nanoscale, 2015, 7, 20709-20716.	2.8	19
226	Color resolution improvement of the dark-field microscopy imaging of single light scattering plasmonic nanoprobes for microRNA visual detection. Nanoscale, 2017, 9, 4593-4600.	2.8	19
227	Tb-containing metal-organic gel with high stability for visual sensing of nitrite. Materials Letters, 2018, 211, 157-160.	1.3	19
228	Dy(III)-induced aggregation emission quenching effect of single-layered graphene quantum dots for selective detection of phosphate in the artificial wetlands. Talanta, 2019, 196, 100-108.	2.9	19
229	Nucleolin-Targeted DNA Nanotube for Precise Cancer Therapy through Förster Resonance Energy Transfer-Indicated Telomerase Responsiveness. Analytical Chemistry, 2021, 93, 3526-3534.	3.2	19
230	Aggregation-Enhanced Energy Transfer for Mitochondria-Targeted ATP Ratiometric Imaging in Living Cells. Analytical Chemistry, 2021, 93, 11878-11886.	3.2	19
231	A ratiometric fluorescence recognition of guanosine triphosphate on the basis of Zn(ii) complex of 1,4-bis(imidazol-1-ylmethyl) benzene. Analyst, The, 2012, 137, 5291.	1.7	18
232	Sensitive and selective turn off-on fluorescence detection of heparin based on the energy transfer platform using the BSA-stabilized Au nanoclusters/amino-functionalized graphene oxide hybrids. Talanta, 2016, 161, 482-488.	2.9	18
233	Co-metal-organic-frameworks with pure uniform crystal morphology prepared via Co2+ exchange-mediated transformation from Zn-metallogels for luminol catalysed chemiluminescence. Spectrochimica Acta - Part A: Molecular and Biomolecular Spectroscopy, 2017, 175, 11-16.	2.0	18
234	Dimension conversion: from a 1D metal–organic gel into a 3D metal–organic porous network with high-efficiency multiple enzyme-like activities for cascade reactions. Nanoscale Horizons, 2020, 5, 119-123.	4.1	18

#	Article	IF	CITATIONS
235	A rapid and sensitive spectrofluorometric method for 6-mercaptopurine using CdTe quantum dots. Analytical Methods, 2013, 5, 673-677.	1.3	17
236	A visual physiological temperature sensor developed with gelatin-stabilized luminescent silver nanoclusters. Talanta, 2015, 143, 469-473.	2.9	17
237	Coomassie brilliant blue R-250 as a new surface-enhanced Raman scattering probe for prion protein through a dual-aptamer mechanism. Talanta, 2015, 139, 35-39.	2.9	17
238	Time-resolved visual detection of heparin by accelerated etching of gold nanorods. Analyst, The, 2018, 143, 824-828.	1.7	17
239	The localized surface plasmon resonance induced edge effect of gold regular hexagonal nanoplates for reaction progress monitoring. Chemical Communications, 2018, 54, 13359-13362.	2.2	17
240	Inconspicuous Reactions Identified by Improved Precision of Plasmonic Scattering Dark-Field Microscopy Imaging Using Silver Shell-Isolated Nanoparticles as Internal References. Analytical Chemistry, 2019, 91, 3002-3008.	3.2	17
241	Indole Carbonized Polymer Dots Boost Full-Color Emission by Regulating Surface State. IScience, 2020, 23, 101546.	1.9	17
242	Discrimination of copper and silver ions based on the label-free quantum dots. Talanta, 2020, 220, 121430.	2.9	17
243	Microscopic determination of tetracycline based on aluminum-sensitized fluorescence of a self-ordered ring formed by a sessile droplet on glass slide support. Journal of Pharmaceutical and Biomedical Analysis, 2004, 34, 103-114.	1.4	16
244	Digitized single scattering nanoparticles for probing molecular binding. Chemical Communications, 2013, 49, 8262.	2.2	16
245	Potassium-induced G-quadruplex DNAzyme as a chemiluminescent sensing platform for highly selective detection of K ⁺ . Analytical Methods, 2014, 6, 7415-7419.	1.3	16
246	Controllable preparation of graphene oxide/metal nanoparticle hybrids as surface-enhanced Raman scattering substrates for 6-mercaptopurine detection. RSC Advances, 2014, 4, 16327-16332.	1.7	16
247	Neural Activation during Anticipation of Near Pain-Threshold Stimulation among the Pain-Fearful. Frontiers in Neuroscience, 2016, 10, 342.	1.4	16
248	A dynamic cell entry pathway of respiratory syncytial virus revealed by tracking the quantum dot-labeled single virus. Nanoscale, 2017, 9, 7880-7887.	2.8	16
249	Aptamer-modified selenium nanoparticles for dark-field microscopy imaging of nucleolin. Chemical Communications, 2017, 53, 13047-13050.	2.2	16
250	Self-Healing 3D Liquid Freestanding Plasmonic Nanoparticle Membrane for Reproducible Surface-Enhanced Raman Spectroscopy Sensing. ACS Applied Nano Materials, 2020, 3, 10014-10021.	2.4	16
251	Microscopic electron counting during plasmon-driven photocatalytic proton coupled electron transfer on a single silver nanoparticle. Applied Catalysis B: Environmental, 2021, 291, 120090.	10.8	16
252	Structure-Guided Designing Pre-Organization in Bivalent Aptamers. Journal of the American Chemical Society, 2022, 144, 4507-4514.	6.6	16

#	Article	IF	CITATIONS
253	Facile synthesis of porphyrin-MOFs with high photo-Fenton activity to efficiently degrade ciprofloxacin. Journal of Colloid and Interface Science, 2022, 622, 690-699.	5.0	16
254	Determination of Proteins with Ponceau G by Compensating for the Molecular Absorption Decreased Resonance Light Scattering Signals. Analytical Letters, 2003, 36, 1557-1571.	1.0	15
255	An Efficient and Selective Deprotecting Method for Methoxymethyl Ethers. Synthetic Communications, 2004, 34, 4325-4330.	1.1	15
256	Light scattering investigations on mercury ion induced amalgamation of gold nanoparticles in aqueous medium. Science China Chemistry, 2012, 55, 1445-1450.	4.2	15
257	In situ labelling chemistry of respiratory syncytial viruses by employing the biotinylated host-cell membrane protein for tracking the early stage of virus entry. Chemical Communications, 2014, 50, 15776-15779.	2.2	15
258	Dopamine derived copper nanocrystals used as an efficient sensing, catalysis and antibacterial agent. RSC Advances, 2015, 5, 55832-55838.	1.7	15
259	Insight into a reversible energy transfer system. Nanoscale, 2016, 8, 16236-16242.	2.8	15
260	Large-scale preparation of fernwort-like single-crystalline superstructures of CuSe as Fenton-like catalysts for dye decolorization. Science China Chemistry, 2016, 59, 903-909.	4.2	15
261	His-tag based in situ labelling of progeny viruses for real-time single virus tracking in living cells. Nanoscale, 2016, 8, 18635-18639.	2.8	15
262	A portable multi-channel sensing device using Au nano-urchins as probes for melamine detection in milk. Journal of Materials Chemistry C, 2017, 5, 7806-7812.	2.7	15
263	A single gold nanoprobe for colorimetric detection of silver(<scp>i</scp>) ions with dark-field microscopy. Analyst, The, 2019, 144, 2011-2016.	1.7	15
264	Dual-aptamer-based sensitive and selective detection of prion protein through the fluorescence resonance energy transfer between quantum dots and graphene oxide. Analytical Methods, 2013, 5, 6904.	1.3	14
265	Selective and sensitive colorimetric detection of stringent alarmone ppGpp with Fenton-like reagent. Analyst, The, 2014, 139, 6284-6289.	1.7	14
266	Visual Identification of Light-Driven Breakage of the Silver-Dithiocarbamate Bond by Single Plasmonic Nanoprobes. Scientific Reports, 2015, 5, 15427.	1.6	14
267	A magnetic nanoparticle-based aptasensor for selective and sensitive determination of lysozyme with strongly scattering silver nanoparticles. Analyst, The, 2016, 141, 3020-3026.	1.7	14
268	Heparin sodium-selective â€~on–off' and lysine-selective â€~off–on' fluorescence switching of cadmited telluride quantum dots and their analytical applications. Analytical Methods, 2016, 8, 453-459.	um 1.3	14
269	Sensitive detection of respiratory syncytial virus based on a dual signal amplified plasmonic enzyme-linked immunosorbent assay. Analytica Chimica Acta, 2017, 962, 73-79.	2.6	14
270	Enzymeâ€ŧriggered fluorescence turnâ€off/turnâ€on of carbon dots for monitoring βâ€glucosidase and its inhibitor in living cells. Luminescence, 2020, 35, 222-230.	1.5	14

#	Article	IF	CITATIONS
271	Efficient peroxydisulfate electrochemiluminescence system based the novel silver metal-organic gel as an effective enhancer. Electrochimica Acta, 2020, 357, 136842.	2.6	14
272	Nanofabrication of hollowed-out Au@AgPt core-frames <i>via</i> selective carving of silver and deposition of platinum. Chemical Communications, 2020, 56, 2945-2948.	2.2	14
273	In situ investigating the size-dependent scattering signatures and sensing sensitivity of single silver nanocube through a multi-model approach. Journal of Colloid and Interface Science, 2021, 584, 253-262.	5.0	14
274	Facile one-pot synthesis of folic acid-modified graphene to improve the performance of graphene-based sensing strategy. Journal of Colloid and Interface Science, 2014, 426, 293-299.	5.0	13
275	Visual and light scattering spectrometric method for the detection of melamine using uracil 5′-triphosphate sodium modified gold nanoparticles. Spectrochimica Acta - Part A: Molecular and Biomolecular Spectroscopy, 2017, 173, 99-104.	2.0	13
276	Highly sensitive detection of hepatitis C virus DNA by using a one-donor-four-acceptors FRET probe. Talanta, 2018, 185, 118-122.	2.9	13
277	The synergistic effect enhanced chemical etching of gold nanorods for the rapid and sensitive detection of biomarks. Talanta, 2020, 219, 121203.	2.9	13
278	Weak Reaction Scatterometry of Plasmonic Resonance Light Scattering with Machine Learning. Analytical Chemistry, 2021, 93, 12131-12138.	3.2	13
279	One-component nano-metal-organic frameworks with superior multienzyme-mimic activities for 1,4-dihydropyridine metabolism. Journal of Colloid and Interface Science, 2022, 605, 214-222.	5.0	13
280	Chirality transfer of cysteine to the plasmonic resonance region through silver coating of gold nanobipyramids. Chemical Communications, 2021, 57, 3211-3214.	2.2	13
281	Plasmonic biosensor for the highly sensitive detection of microRNA-21 via the chemical etching of gold nanorods under a dark-field microscope. Biosensors and Bioelectronics, 2022, 201, 113942.	5.3	13
282	Quantitation and Differentiation of Bioparticles Based on the Measurements of Light-Scattering Signals with a Common Spectrofluorometer. Journal of Physical Chemistry B, 2008, 112, 11785-11793.	1.2	12
283	Nonstoichiometric Cu _{2â^'x} Se nanocrystals in situ produced on the surface of carbon nanotubes for ablation of tumor cells. New Journal of Chemistry, 2016, 40, 6315-6324.	1.4	12
284	Distance-Dependence Study of Plasmon Resonance Energy Transfer with DNA Spacers. Analytical Chemistry, 2020, 92, 14278-14283.	3.2	12
285	Resonance light scattering technique for sensitive detection of heparin using plasmonic Cu2-xSe nanoparticles. Talanta, 2020, 216, 120967.	2.9	12
286	Catalytic hairpin assembled polymeric tetrahedral DNA frameworks for MicroRNA imaging in live cells. Biosensors and Bioelectronics, 2022, 197, 113783.	5.3	12
287	Formation of blue fluorescent ribbons of 4′,4′′′′a€²-(1,4-phenylene)bis(2,2′:6′,2′′-terpyrid visual detection of iron(<scp>ii</scp>) cations. RSC Advances, 2013, 3, 111-116.	ine) and hi 1.7	ghly select ve
288	A plasmon resonance light scattering assay of glucose based on the formation of gold nanoparticles. Analytical Methods, 2014, 6, 3779-3783.	1.3	11

#	Article	IF	CITATIONS
289	Theoretical investigations on enhancing the performance of terminally diketopyrrolopyrrole-based small-molecular donors in organic solar cell applications. Journal of Molecular Modeling, 2016, 22, 15.	0.8	11
290	Visual detection of cancer cells by using <i>in situ</i> grown functional Cu _{2â^x} Se/reduced graphene oxide hybrids acting as an efficient nanozyme. Analyst, The, 2019, 144, 716-721.	1.7	11
291	Current diagnostic and therapeutic strategies for COVID-19. Journal of Pharmaceutical Analysis, 2021, 11, 129-137.	2.4	11
292	Telomerase Activity Assay via 3,3′,5,5′-Tetramethylbenzidine Dilation Etching of Gold Nanorods. ACS Applied Nano Materials, 2022, 5, 1484-1490.	2.4	11
293	Sensitive Logic Nanodevices with Strong Response for Weak Inputs. Angewandte Chemie - International Edition, 2022, 61, .	7.2	11
294	Dual-aptamer-based enzyme linked plasmonic assay for pathogenic bacteria detection. Colloids and Surfaces B: Biointerfaces, 2022, 214, 112471.	2.5	11
295	Gold nanoparticles based digital color analysis for quinidine detection. Science Bulletin, 2013, 58, 2027-2031.	1.7	10
296	Vertically aligned gold nanomushrooms on graphene oxide sheets as multifunctional nanocomposites with enhanced catalytic, photothermal and SERS properties. RSC Advances, 2016, 6, 93645-93648.	1.7	10
297	An ultrathin 2D Yb(III) metal-organic frameworks with strong electrochemiluminescence as a "on-off-on―platform for detection of picric acid and berberine chloride form. Talanta, 2021, 234, 122625.	2.9	10
298	DNA Logic Nanodevices for Real-Time Monitoring of ATP in Lysosomes. Analytical Chemistry, 2021, 93, 15331-15339.	3.2	10
299	Energy Flow during the Plasmon Resonance-Driven Photocatalytic Reactions on Single Nanoparticles. ACS Catalysis, 2022, 12, 847-853.	5.5	10
300	Observation of the Unusual Aggregation Kinetics of Colloidal Minerals in Acidic Solutions. Journal of Chemical Sciences, 2015, 127, 1083-1089.	0.7	9
301	Facile synthesis of gold nanoflowers as SERS substrates and their morphological transformation induced by iodide ions. Science China Chemistry, 2016, 59, 1045-1050.	4.2	9
302	Catalytic chemiluminescent detection of cholesterol in serum with Cu2â^'x Se semiconductor nanoparticles. Analytical and Bioanalytical Chemistry, 2016, 408, 8771-8778.	1.9	9
303	Nonstoichiometric copper chalcogenides for photo-activated alkyne/azide cycloaddition. Physical Chemistry Chemical Physics, 2017, 19, 6964-6968.	1.3	9
304	Rapid detection of heparin by gold nanorods and near-infrared fluorophore ensemble based platform via nanometal surface energy transfer. Sensors and Actuators B: Chemical, 2018, 274, 318-323.	4.0	9
305	Catalytic hairpin assembly mediated liposome-encoded magnetic beads for signal amplification of peroxide test strip based point-of-care testing of ricin. Chemical Communications, 2020, 56, 14091-14094.	2.2	9
306	Nanosurface energy transfer indicating Exo III-propelled stochastic 3D DNA walkers for HIV DNA detection. Analyst, The, 2021, 146, 1675-1681.	1.7	9

#	Article	IF	CITATIONS
307	A crosslinked submicro-hydrogel formed by DNA circuit-driven protein aggregation amplified fluorescence anisotropy for biomolecules detection. Analytica Chimica Acta, 2021, 1154, 338319.	2.6	9
308	Europium coordination polymer particles based electrospun nanofibrous film for point-of-care testing of copper (II) ions. Talanta, 2021, 228, 122270.	2.9	9
309	Rational fabrication of a DNA walking nanomachine on graphene oxide surface for fluorescent bioassay. Biosensors and Bioelectronics, 2022, 211, 114349.	5.3	9
310	Highly selective recognition of adenosine 5′-triphosphate against other nucleosides triphosphate with a luminescent metal-organic framework of [Zn(BDC)(H2O)2] n (BDC = 1,4-benzenedicarboxylate). Science China Chemistry, 2013, 56, 1651-1657.	4.2	8
311	Multifunctional fluorescent carbon dots inhibit the invasiveness of lung cancer cells. New Journal of Chemistry, 2018, 42, 15311-15314.	1.4	8
312	Multifunctional Single-Layered Graphene Quantum Dots Used for Diagnosis of Mitochondrial Malfunction-Related Diseases. ACS Biomaterials Science and Engineering, 2020, 6, 1727-1734.	2.6	8
313	Long-distance transfer of plasmonic hot electrons across the Au–Pt porous interface for the hydrogen evolution reaction. Journal of Materials Chemistry C, 2021, 9, 3108-3114.	2.7	8
314	Lighting up of carbon dots for copper(<scp>ii</scp>) detection using an aggregation-induced enhanced strategy. Analyst, The, 2022, 147, 417-422.	1.7	8
315	"Hepatitis virus indicatorâ€⊷-the simultaneous detection of hepatitis B and hepatitis C viruses based on the automatic particle enumeration. Biosensors and Bioelectronics, 2022, 202, 114001.	5.3	8
316	A catalyst-free co-reaction system of long-lasting and intensive chemiluminescence applied to the detection of alkalineAphosphatase. Mikrochimica Acta, 2022, 189, 181.	2.5	8
317	Determination of Heparin Using Azure B by Flow Injection Analysisâ€Resonance Light Scattering Coupled Technique. Analytical Letters, 2005, 38, 317-330.	1.0	7
318	A facile one-pot method to fabricate gold nanoparticle chains with dextran. Science China Chemistry, 2013, 56, 387-392.	4.2	7
319	Single scattering particles based analytical techniques. Science Bulletin, 2013, 58, 1969-1979.	1.7	7
320	Metal-Mediated Gold Nanospheres Assembled for Dark-Field Microscopy Imaging Scatterometry. Talanta, 2019, 201, 280-285.	2.9	7
321	High Resolution of Plasmonic Resonance Scattering Imaging with Deep Learning. Analytical Chemistry, 2022, 94, 4610-4616.	3.2	7
322	Pharmacokinetic detection of penicillin excreted in urine using a totally internally reflected resonance light scattering technique with cetyltrimethylammonium bromide. Analytical and Bioanalytical Chemistry, 2005, 382, 85-90.	1.9	6
323	Investigations on the amalgamation of gold nanorods by iodine and the detection of tetracycline. Science in China Series B: Chemistry, 2009, 52, 188-195.	0.8	6
324	Homochiral expression of proteins: a discussion on the natural chirality related to the origin of life. Science China Chemistry, 2010, 53, 792-796.	4.2	6

#	Article	IF	CITATIONS
325	Determination of heparin based on the reaction with Co(ii)/5-Cl-PADAB complex using the resonance Rayleigh scattering technology. Analytical Methods, 2013, 5, 2511.	1.3	6
326	Facile synthesis of hierarchical metal–organic microsheet-assembled microflowers. Materials Letters, 2015, 152, 139-141.	1.3	6
327	A new spectrofluorometric method for pyrophosphate assay based on the fluorescence enhancement of trypsin-stabilized copper clusters. Analytical Methods, 2015, 7, 638-642.	1.3	6
328	Magnetic Bead-Based Sandwich Immunoassay for Viral Pathogen Detection by Employing Gold Nanoparticle as Carrier. Journal of Analysis and Testing, 2017, 1, 298-305.	2.5	6
329	Rational Design of pHâ€Responsive DNA Motifs with General Sequence Compatibility. Angewandte Chemie, 2019, 131, 16557-16562.	1.6	6
330	Metalâ€Organic Gelâ€Derived Co/CoO/Co 3 O 4 Composite for the Electrochemical Detection of Diethylstilbestrol. Applied Organometallic Chemistry, 2020, 34, e5536.	1.7	6
331	Homo-FRET enhanced ratiometric fluorescence strategy for exonuclease III activity detection. Analytical Methods, 2021, 13, 1489-1494.	1.3	6
332	Size-Dependent Plasmonic Resonance Scattering Characteristics of Gold Nanorods for Highly Sensitive Detection of microRNA-27a. ACS Applied Bio Materials, 2021, 4, 3469-3475.	2.3	6
333	DNA Photonic Nanowires for Homogeneous Entropy-Driven Biomolecular Assay of Thrombin. ACS Applied Nano Materials, 2021, 4, 2849-2854.	2.4	6
334	Preparation of a molecularly imprinted test strip for point-of-care detection of thiodiglycol, a sulfur mustard poisoning metabolic marker. Talanta, 2021, 234, 122701.	2.9	6
335	A high-integrated DNA biocomputing platform for MicroRNA sensing in living cells. Biosensors and Bioelectronics, 2022, 207, 114183.	5.3	6
336	Pork Heart Tissueâ€Based Chemiluminescence Biosensor for Pyruvic Acid. Analytical Letters, 2006, 39, 1823-1836.	1.0	5
337	Polarized synchronous light scattering characterization of the interaction of proteins with sodium dodecyl sulfonate. Science Bulletin, 2007, 52, 456-460.	1.7	5
338	Controllable synthesis of polyoxometalates nanocubes and their specific interactions with prion proteins. Science in China Series B: Chemistry, 2009, 52, 2156-2160.	0.8	5
339	Orientation-independent reaction activity monitoring with single particle and data analytics. Journal of Colloid and Interface Science, 2021, 590, 458-466.	5.0	5
340	FRET-enhanced nanoflares for sensitive and rapid detection of ampicillin. Analytical Methods, 2020, 12, 970-976.	1.3	5
341	Au Nanoparticle-Based Fluorescent Turn-on Nanoprobes for Real-Time Imaging the Expression of miR-630 during Cell Apoptosis. ACS Applied Nano Materials, 2021, 4, 13469-13476.	2.4	5
342	A centrifugal microfluidic chip for point-of-care testing of staphylococcal enterotoxin B in complex matrices. Nanoscale, 2022, 14, 1380-1385.	2.8	5

#	Article	IF	CITATIONS
343	A backscattering light detection assembly for sensitive determination of analyte concentrated at the liquid/liquid interface using the interaction of quercetin with proteins as the model system. Analyst, The, 2005, 130, 200.	1.7	4
344	Multi-walled carbon nanotubes based catalyst plasmon resonance light scattering analysis of tetracycline hydrochloride. Science in China Series B: Chemistry, 2008, 51, 866-871.	0.8	4
345	Investigations of the interaction between cuprous oxide nanoparticles and Staphylococcus aureus. Science in China Series B: Chemistry, 2009, 52, 1028-1032.	0.8	4
346	Raman scattering detection of cobalt(ii) ions based on their specific etching effect on leaf-like poly(p-phenylenediamine) microcrystals. Analytical Methods, 2014, 6, 5054.	1.3	4
347	H ₂ S bubbles-assisted synthesis of hollow Cu _{2â~x} Se _y S _{1â~'y} /reduced graphene oxide nanocomposites with tunable compositions and localized surface plasmon resonance. RSC Advances, 2015, 5, 91206-91212.	1.7	4
348	A study of the catalytic ability of in situ prepared AgNPs–PMAA–PVP electrospun nanofibers. New Journal of Chemistry, 2015, 39, 9518-9524.	1.4	4
349	A label-free turn ON–OFF chemiluminescence strategy for lysozyme detection by target-triggered Cu _{2â~'x} Se aggregation. Analytical Methods, 2019, 11, 4376-4381.	1.3	4
350	DNA nanosheet as an excellent fluorescence anisotropy amplification platform for accurate and sensitive biosensing. Talanta, 2020, 211, 120730.	2.9	4
351	Direct visualization of photo-induced disulfide through oxidative coupling of <i>para</i> -aminothiophenol. Chemical Communications, 2021, 57, 4190-4193.	2.2	4
352	Soft nanoball-encapsulated carbon dots for reactive oxygen species scavenging and the highly sensitive chemiluminescent assay of nucleic acid biomarkers. Analyst, The, 2021, 146, 7187-7193.	1.7	4
353	Functional molecules and nano-materials for the Golgi apparatus-targeted imaging and therapy. TrAC - Trends in Analytical Chemistry, 2022, 156, 116714.	5.8	4
354	DETERMINATION OF TRACE AMOUNT OF ALUMINUM IN WATER SAMPLES BY A FLUORESCENT MICROSCOPIC SELF-ORDERED RING TECHNIQUE. Analytical Letters, 2002, 35, 2565-2576.	1.0	3
355	The adsorption of silver nanoparticles on the proteins-immobilized glass slides and a visual investigation on proteins immobilization. Science in China Series B: Chemistry, 2009, 52, 639-643.	0.8	3
356	Pharmacia and biological functionalities of nutrient broth dispersed multi-walled carbon nanotubes: A novel drug delivery system. Science China Chemistry, 2010, 53, 612-618.	4.2	3
357	Theoretical Investigations on Naphthodithiophene Diimideâ€Based Copolymers as Acceptor for Allâ€Polymer Solar Cell Applications. ChemistrySelect, 2016, 1, 1662-1673.	0.7	3
358	Glutathione-driven Cu(<scp>i</scp>)–O ₂ chemistry: a new light-up fluorescent assay for intracellular glutathione. Analyst, The, 2018, 143, 2486-2490.	1.7	3
359	Ultrasonic one-step synthesis of biocompatible yellow-green fluorescent carbon dots. Scientia Sinica Chimica, 2013, 43, 895-900.	0.2	3
360	Arsenic Trioxide and Artemisinin Act Synergistically to Kill Tumor Cells In Vitro. Anti-Cancer Agents in Medicinal Chemistry, 2019, 18, 2178-2186.	0.9	3

#	Article	IF	CITATIONS
361	One-donor-two-acceptors coupled energy transfer nanoprobe for recording of viral gene replication in living cells. Chemical Engineering Journal, 2022, 434, 134658.	6.6	3
362	The restructure of Au@Ag nanorods for cell imaging with dark-field microscope. Talanta, 2022, 244, 123403.	2.9	3
363	Resonance Light Scattering Method to Determine Binding Ratio and Functional Affinity Constant of Antigen/Antibody Immunoreaction. Analytical Letters, 2009, 42, 1495-1508.	1.0	2
364	Tetrakis(4-sulfonatophenyl)porphyrin-Directed Assembly of Gold Nanocrystals: Tailoring the Plasmon Coupling Through Controllable Gap Distances. Small, 2010, 6, n/a-n/a.	5.2	2
365	Cellular prion protein imaging analysis with aptamer-labeled Ru(bpy) 3 2+ -doped silica nanoparticles. Science Bulletin, 2014, 59, 147-153.	1.7	2
366	Hybridization chain reaction triggered controllable one-dimensional assembly of gold nanoparticles. Science China Chemistry, 2016, 59, 1513-1518.	4.2	2
367	ZnO micron rods as single dielectric resonator for optical sensing. Analytica Chimica Acta, 2020, 1109, 107-113.	2.6	2
368	Gold triangular nanoplates with edge effect for reaction monitoring under dark-field microscopy. Colloids and Surfaces A: Physicochemical and Engineering Aspects, 2022, 647, 129133.	2.3	2
369	Fluorescence turn-on Cu2-xSe@HA-rhodamine 6G FRET nanoprobe for hyaluronidase detection and imaging. Journal of Photochemistry and Photobiology B: Biology, 2022, 233, 112496.	1.7	2
370	Preparation of carbon dots and their sensing applications. , 2022, , 9-40.		1
371	Sensitive Logic Nanodevices with Strong Response for Weak Inputs. Angewandte Chemie, 0, , .	1.6	1
372	Programmable, Universal DNAzyme Amplifier Supporting Pancreatic Cancer-Related miRNAs Detection. Chemosensors, 2022, 10, 276.	1.8	1
373	Theoretical Investigation of Donor–Acceptor Copolymers Based on C-, Si-, and Ge-Bridged Thieno[3,2-b]dithiophene for Organic Solar Cell Applications. Journal of Electronic Materials, 2016, 45, 5427-5435.	1.0	0
374	Characteristics of DNA-AuNP networks on cell membranes and real-time movies for viral infection. Data in Brief, 2016, 6, 652-660.	0.5	0
375	Preparation and structure tuning of graphene quantum dots for optical applications in chemosensing, biosensing, and bioimaging. , 2022, , 41-77.		0
376	Synthesis, functionalization, and optical sensing applications of graphene oxide. , 2022, , 79-118.		0
377	Cationic conjugated polymer-based FRET aptasensor for label-free and ultrasensitive ractopamine detection. RSC Advances, 2022, 12, 10911-10914.	1.7	0